PHYSICAL REVIEW B **88**, 201405(R) (2013)

Charge-carrier-induced frequency renormalization, damping, and heating of vibrational modes in nanoscale junctions

Kristen Kaasbjerg,[1,*] Tomáš Novotný,[2] and Abraham Nitzan[1]

[1]*School of Chemistry, The Sackler Faculty of Exact Sciences, Tel Aviv University, Tel Aviv 69978, Israel*

[2]*Department of Condensed Matter Physics, Faculty of Mathematics and Physics, Charles University in Prague, Ke Karlovu 5, 12116 Prague, Czech Republic*

(Received 27 April 2013; revised manuscript received 29 October 2013; published 20 November 2013)

In nanoscale junctions the interaction between charge carriers and the local vibrations results in renormalization, damping, and heating of the vibrational modes. Here we formulate a nonequilibrium Green's function based theory to describe such effects. Studying a generic junction model with an off-resonant electronic level, we find a strong bias dependence of the frequency renormalization and vibrational damping accompanied by pronounced nonlinear vibrational heating in junctions with intermediate values of the coupling to the leads. Combining our theory with *ab initio* calculations, we furthermore show that the bias dependence of the Raman shifts and linewidths observed experimentally in an oligo(3)-phenylenevinylene (OPV3) junction [Ward *et al.*, Nat. Nanotechnol. **6**, 33 (2011)] may be explained by a combination of dynamic carrier screening and molecular charging.

DOI: 10.1103/PhysRevB.88.201405 PACS number(s): 73.23.−b, 71.38.−k, 85.65.+h

Introduction. A fundamental understanding of the nonequilibrium behavior of the atomic degrees of freedom in current-carrying nanoscale junctions is of major importance for the realization of molecule-based electronics. Joule heating arising from the interaction between the electronic charge carriers and the molecular vibrations has been observed experimentally[1–4] and poses a serious stability issue in such junctions.

The implications of the electron-vibration (el-vib) interaction on both the current and heating in molecular junctions have been the subject of intense theoretical studies,[5] and critical effects such as vibrational instabilities[6,7] and cooling mechanisms[8–10] have been addressed. In addition, recent developments[11–14] have demonstrated the existence of nonconservative current-induced forces that can drive the molecular vibrations strongly out of equilibrium and provide further channels for junction destabilization. Efforts to identify vibrational heating and instabilities in, e.g., inelastic-tunneling spectroscopy (IETS),[15] current noise,[16,17] and Raman spectroscopy[14,18,19] are still ongoing.

Raman spectroscopy on current-carrying molecular junctions[3,4] offers a unique diagnostic tool for monitoring the nonequilibrium behavior of the molecular vibrations. Apart from the information about heating encoded in the Stokes/anti-Stokes ratio, Raman spectroscopy provides direct access to the vibrational spectral function of the molecule. Experimentally, this has revealed noticeable frequency shifts and broadenings of the vibrations as a function of bias voltage.[4] Similar effects originating from the electron-phonon interaction are well known from, e.g., Raman spectroscopy on gated graphene[20,21] and current-carrying nanomechanical carbon-nanotube resonators,[22–25] and provide useful insight into the mechanisms governing vibrational damping and heat dissipation in such systems.

In this Rapid Communication we study these effects in nanoscale atomic/molecular junctions where nonadiabatic (dynamic) effects become important when the electronic and vibrational energy scales are comparable. For this purpose, we formulate a nonequilibrium Green's function (NEGF) based theory for vibrational frequency renormalization and heating, taking into account electronic charging and screening effects on the local junction vibrations. We find that (i) strong bias-dependent frequency renormalization and damping is accompanied by pronounced nonlinear bias-dependent heating, and (ii) the above-mentioned carrier-related mechanisms may explain the voltage dependence of the Raman shifts and linewidths observed in Ref. 4.

Theory. To address the effect of carrier-induced renormalization and heating of vibrations in biased nanoscale junctions, we employ the NEGF,[26] which treats the dynamics of the electronic and vibrational degrees of freedom on equal footing.[27,28] In the general case with more than one local junction vibration, the dressed vibrational retarded Green's

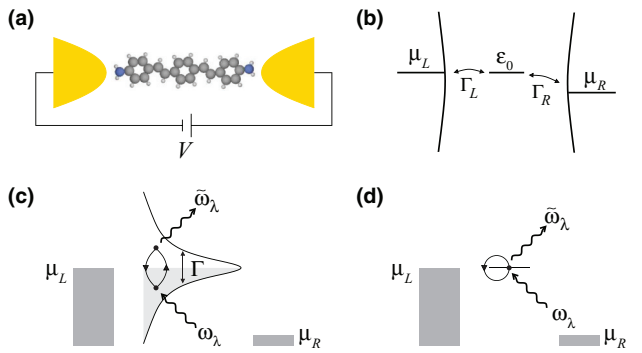

FIG. 1. (Color online) (a) Molecular contact with an amine-terminated (NH_2) OPV3 molecule sandwiched between the source and drain electrodes. (b) Generic junction description in terms of a single molecular level ε_0 with lead-induced broadening $\Gamma = \Gamma_L + \Gamma_R$ and applied bias voltage $eV = \mu_R - \mu_L$. (c), (d) Processes responsible for the carrier-induced renormalization of vibrational frequencies ($\omega_\lambda \to \tilde{\omega}_\lambda$) and electron-hole damping ($\gamma_\lambda^{\mathrm{eh}}$). The illustrations correspond to the Feynman diagrams for the self-energies in Eqs. (2) and (3), respectively, describing the dynamic renormalization via *virtual* electron-hole pairs (screening) (c) and the static renormalization due to (partial) charging of the level (d).

function (GF) is given in the matrix form as

$$\mathbf{D}^r(\omega) = \left\{\left[\mathbf{D}_0^r(\omega)\right]^{-1} - \mathbf{\Pi}^r(\omega)\right\}^{-1}, \tag{1}$$

where $\mathbf{D}_0^r(\omega)$ is the bare diagonal GF given by $D_{0,\lambda}^r(\omega) = 2\omega_\lambda/[(\omega+i0^+)^2-\omega_\lambda^2]$ for the vibrational mode λ with frequency ω_λ, and the spectral function is given by the imaginary part of retarded GF as $A(\omega) = -2\sum_\lambda \mathrm{Im}\, D_{\lambda\lambda}^r(\omega)$. The vibrational self-energy $\Pi = \Pi^{\mathrm{el}} + \Pi^{\mathrm{ph}}$ in general has contributions from both the interaction with electronic charge carriers (Π^{el}) and phonon-related effects (Π^{ph}).[29] The latter, reflecting coupling to environmental phonons as well as anharmonicity,[30–33] is described here by a phenomenological damping rate γ_{ph} (see, e.g., Ref. 28) which does not affect the vibrational frequencies.

For the electronic part of the self-energy, we consider a junction where the transport is dominated by a single electronic level [highest occupied molecular orbital (HOMO) or lowest unoccupied molecular orbital (LUMO)] with energy ε_0 and level broadening $\Gamma = \Gamma_L + \Gamma_R$ due to the leads [see Fig. 1(b)]. The level is coupled to the local vibrations via linear $H^{(1)} = n_0\sum_\lambda M_\lambda^{(1)}(a_\lambda^\dagger + a_\lambda)$ and quadratic $H^{(2)} = \frac{1}{2}n_0\sum_{\lambda\lambda'}(a_\lambda^\dagger + a_\lambda)M_{\lambda\lambda'}^{(2)}(a_{\lambda'}^\dagger + a_{\lambda'})$ el-vib interaction terms, where $n_0 = n_\uparrow + n_\downarrow$ is the level occupancy and $M_\lambda^{(1)}$ ($M_{\lambda\lambda'}^{(2)}$) the linear (quadratic) el-vib coupling. The retarded components of the electronic self-energy $\Pi^{\mathrm{el}} = \Pi^{(1)} + \Pi^{(2)}$ are to the lowest (nonzero) order given by the electronic polarizability[28]

$$\Pi_{\lambda\lambda'}^{(1),r}(\omega) = -2i\int\frac{d\varepsilon}{2\pi}\left[M_\lambda^{(1)}G^r(\varepsilon)M_{\lambda'}^{(1)}G^<(\varepsilon-\omega) + M_\lambda^{(1)}G^<(\varepsilon)M_{\lambda'}^{(1)}G^a(\varepsilon-\omega)\right], \tag{2}$$

and the level occupancy[34]

$$\Pi_{\lambda\lambda'}^{(2),r}(\omega) = -2iM_{\lambda\lambda'}^{(2)}\int\frac{d\varepsilon}{2\pi}G^<(\varepsilon) = \langle n_0\rangle M_{\lambda\lambda'}^{(2)}, \tag{3}$$

respectively, where the factors of 2 account for spin degeneracy. The two self-energies, which are illustrated in Figs. 1(c) and 1(d) by their respective Feynman diagrams, account for frequency renormalization due to dynamic screening and static (partial) charging, respectively. In addition, the former also accounts for spectral broadening due to damping by electron-hole (eh) pair excitations.

Vibrational heating originates from the linear el-vib interaction and can be quantified in terms of the nonequilibrium occupation $\tilde{n}_\lambda$ of the renormalized vibration. As we show here in detail,[34] the physically relevant (i.e., experimentally verifiable via, e.g., Raman spectroscopy) occupation factor for a renormalized vibration is given by

$$\tilde{n}_\lambda = -\frac{1}{2} + \frac{\tilde{\omega}_\lambda}{\omega_\lambda}\frac{i}{2}\int\frac{d\omega}{2\pi}D_{\lambda\lambda}^<(\omega), \tag{4}$$

where $\tilde{\omega}_\lambda$ is the renormalized frequency, $D_{\lambda\lambda}^<$ are the diagonal elements of the vibrational lesser GF, $\mathbf{D}^<(\omega) = \mathbf{D}^r(\omega)\mathbf{\Pi}^<(\omega)\mathbf{D}^a(\omega)$, and the *mode-renormalization* factor $\tilde{\omega}_\lambda/\omega_\lambda$ accounts for the renormalization of the field operators $\tilde{a}_\lambda^\dagger + \tilde{a}_\lambda = x_\lambda\sqrt{2\tilde{\omega}_\lambda}$, here related to the vibrational normal coordinate x_λ through the *renormalized* frequency $\tilde{\omega}_\lambda$.

The occupation in Eq. (4) is equivalent to the steady-state solution of the rate equation[34]

$$\dot{\tilde{n}}_\lambda = \left[\gamma_{\mathrm{emis}}^{\mathrm{eh}} + \gamma_{\mathrm{ph}}N_B(\tilde{\omega}_\lambda)\right](\tilde{n}_\lambda+1) - \left[\gamma_{\mathrm{abs}}^{\mathrm{eh}} + \gamma_{\mathrm{ph}}(N_B(\tilde{\omega}_\lambda)+1)\right]\tilde{n}_\lambda, \tag{5}$$

given by

$$\tilde{n}_\lambda = \frac{1}{e^{\hbar\tilde{\omega}_\lambda/k_{\mathrm{B}}T_{\mathrm{eff}}}-1}, \tag{6}$$

where we have introduced an *effective* nonequilibrium mode temperature T_{eff} defined by $e^{\hbar\tilde{\omega}_\lambda/k_{\mathrm{B}}T_{\mathrm{eff}}} = [\gamma_{\mathrm{abs}}^{\mathrm{eh}} + \gamma_{\mathrm{ph}}(N_B+1)]/(\gamma_{\mathrm{emis}}^{\mathrm{eh}} + \gamma_{\mathrm{ph}}N_B)$, $N_B(\omega) = (e^{\hbar\omega/k_{\mathrm{B}}T}-1)^{-1}$ is the Bose-Einstein occupation factor of the environmental phonon bath at temperature T, and $\gamma_{\mathrm{abs}}^{\mathrm{eh}}$ ($\gamma_{\mathrm{emis}}^{\mathrm{eh}}$) is the rate for absorption (emission) of vibrational quanta due to *intra-* and *inter*electrode eh-pair processes [see the inset in Fig. 2(b)]. They can be identified[15] from the eh-pair damping rate $\gamma_\lambda^{\mathrm{eh}} = -2\frac{\omega_\lambda}{\tilde{\omega}_\lambda}\mathrm{Im}\,\Pi_{\lambda\lambda}^{(1),r}(\tilde{\omega}_\lambda)$[34] as $\gamma_\lambda^{\mathrm{eh}} = i\frac{\omega_\lambda}{\tilde{\omega}_\lambda}(\Pi_{\lambda\lambda}^{(1),>} - \Pi_{\lambda\lambda}^{(1),<}) = \gamma_{\mathrm{abs}}^{\mathrm{eh}} - \gamma_{\mathrm{emis}}^{\mathrm{eh}}$. In equilibrium they are related by the detailed balance $\gamma_{\mathrm{emis}}^{\mathrm{eh}} = \gamma_{\mathrm{abs}}^{\mathrm{eh}}\exp(-\frac{\hbar\tilde{\omega}_\lambda}{k_{\mathrm{B}}T})$, implying $T_{\mathrm{eff}} = T$. The total damping rate is given by the imaginary part of the full self-energy as $\gamma_\lambda = -2\frac{\omega_\lambda}{\tilde{\omega}_\lambda}\mathrm{Im}\,\Pi_{\lambda\lambda}^r(\tilde{\omega}_\lambda)$.

In the case of independent vibrations, i.e., when mode-mode couplings given by the off-diagonal elements of the self-energy are negligible, the renormalized frequencies are given by the real part of the self-energy as the solution to the equation

$$\omega^2 = \omega_\lambda^2 + 2\omega_\lambda\,\mathrm{Re}\,\Pi_{\lambda\lambda}^r(\omega), \tag{7}$$

which for small frequency changes $\Delta\omega_\lambda \ll \omega_\lambda$ simplifies to $\Delta\omega_\lambda = \mathrm{Re}\,\Pi_{\lambda\lambda}^r(\omega_\lambda)$. In the limit $\Gamma \gg \omega_\lambda, \varepsilon_0, V$ corresponding to the situation in atomic gold wires,[15,27,35] the renormalization and damping due to the linear el-vib interaction [Eq. (2)] scale as $\Delta\omega_\lambda^{(1)} \sim -(M_\lambda^{(1)})^2/\Gamma = -\omega_\lambda(M_\lambda^{(1)}/\Gamma)^2\Gamma/\omega_\lambda$ and $\gamma_\lambda^{\mathrm{eh}} \sim \omega_\lambda(M_\lambda^{(1)}/\Gamma)^2$, respectively. Even if the dimensionless coupling constant is small $(M_\lambda^{(1)}/\Gamma)^2 \ll 1$, the frequency renormalization may become appreciable if $\Gamma \gg \omega_\lambda$. In this regime, the omission of the *mode renormalization factor* in Eq. (4) has previously led to disagreements between NEGF and rate equation results for the vibrational occupation [see, e.g., Fig. 2(a) of Ref. 36].

In the calculations presented below, we assume low temperature ($T = 0$) and use the *bare* electronic GFs in the evaluation of the self-energies corresponding to the first Born approximation.

Generic junction model. In order to demonstrate the connection between vibrational frequency renormalization, damping, and heating in nanoscale junctions, we start by considering a simple junction with an off-resonant electronic level ε_0 coupled symmetrically to the leads ($\Gamma_L = \Gamma_R$) and interacting weakly with a local vibration with frequency ω_λ. The significance of the electronic energy scales of the junction is illustrated by considering two cases for the lead-induced level broadening representing junctions with $\Gamma \lesssim \varepsilon_0, V$ and $\Gamma \gg \varepsilon_0, V$, respectively (see Fig. 2 for parameters).

In Figs. 2(a) and 2(b) we plot the bias dependence of the renormalized vibrational frequency $\tilde{\omega}_\lambda$ obtained from a self-consistent solution of Eq. (7) and the eh-pair damping rate γ^{eh}, respectively. The qualitatively different bias dependencies in

the two cases stem from different electronic density of states (DOS) of the level. For the largest value of $\Gamma_{L/R}$ in Fig. 2 corresponding to, e.g., break junctions with small molecules,[37] the DOS is low and constant at the scale of the applied bias. The damping is consequently weak ($\gamma^{\rm eh} \lesssim 0.4$ meV) and both the frequency renormalization and damping show very little bias dependence.

When $\Gamma \lesssim \varepsilon_0, V$, the electronic resonance can be introduced into the bias window, resulting in large changes in the level occupancy and the electronic screening with the applied bias. This situation initially results in a softening of the vibration and increased damping with applied bias. At $V = 2\varepsilon_0$, where the level becomes resonant with the chemical potential of the source contact, it is partially filled and therefore has a large DOS for eh-pair excitations [see Fig. 1(c)]. As a consequence, the frequency renormalization and eh-pair damping peak close to this bias voltage value. For higher biases the resonance continues to fill up and eh-pair excitations become suppressed by Pauli blocking [see the inset of Fig. 2(b)]. This results in a subsequent hardening of the frequency, which at high bias saturates at the value given by the charging-induced renormalization $\tilde{\omega}_\lambda = \omega_\lambda + n_0 M_\lambda^{(2)}$, and a strongly reduced damping (see also below).

Next, we consider the heating of the vibration.[38] Figures 2(c) and 2(d) show the bias dependence of the vibrational excitation obtained from Eq. (4) as well as the rate equation result (6), and the elastic current $I = -e\Gamma/h \int d\varepsilon \, \mathrm{Im}\, G^r(\varepsilon)[f_L - f_R]$ through the junction (inelastic contributions are small corrections). Note that the rate-equation and NEGF results are in perfect agreement, as expected. Above the threshold for emission of vibrational quanta at $eV = \hbar\tilde{\omega}_\lambda$ (given by the renormalized frequency) a qualitatively different behavior of the vibrational excitation is observed for the two Γ values. In the $\Gamma \gg \varepsilon_0, V$ case, the linear bias dependence of the vibrational excitation is well known.[15] For $\Gamma \lesssim \varepsilon_0, V$, the bias dependence of the vibrational excitation is strongly nonlinear and, perhaps counterintuitively, experiences stronger (compared to the large Γ case) heating for $V \gtrsim 1.1$ V despite the lower current and stronger damping.

To elucidate the physical origin of the pronounced nonlinear heating in the $\Gamma \lesssim \varepsilon_0, V$ case, we consider the dominant contributions to the eh-pair damping rate from absorption (solid lines) and emission (dashed line) processes shown in the inset of Fig. 2(b). At biases $V > 2\varepsilon_0$, absorption processes with the left lead become Pauli blocked and transport-induced *inter*electrode processes become dominant. Furthermore, when the full resonance is contained in the bias window, i.e., $V \gg \varepsilon_0, \Gamma, \omega_\lambda$, the DOS for absorption and emission processes become comparable, implying that $\gamma^{\rm eh}_{\rm abs} \sim \gamma^{\rm eh}_{\rm emis}$ and $\gamma^{\rm eh} \to 0$. For the steady-state solution (6) this leads ($N_B = 0$ at $T = 0$) to $\tilde{n}_\lambda = \gamma^{\rm eh}_{\rm emis}/\gamma_{\rm ph}$. The bias dependence of the heating thus follows that of the rate for emission processes which is nonlinear due to the Lorentzian broadening of the electronic level and saturates in the high bias limit where the current is carried by the full resonance. This qualitatively explains the pronounced nonlinear heating. It is important to note that the steady-state solution to the rate equation (5) diverges in the high bias limit $V \to \infty$ in the absence of the phonon-related damping parameter $\gamma_{\rm ph}$. This

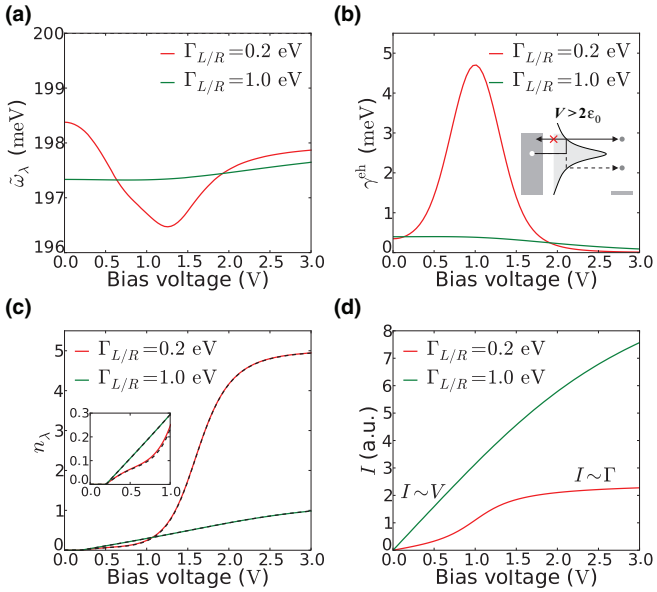

FIG. 2. (Color online) Renormalized frequency $\tilde{\omega}_\lambda$ (a) and electron-hole damping rate $\gamma^{\rm eh} = -2\frac{\omega_\lambda}{\tilde{\omega}_\lambda}\mathrm{Im}\,\Pi^{(1),r}_\lambda(\tilde{\omega}_\lambda)$ (b) as a function of bias voltage V for a vibration interacting with an off-resonant level ($\varepsilon_0 = 0.5$ eV, $\mu_{L/R} = \pm V/2$, $\Gamma_L = \Gamma_R$, $\omega_\lambda = 200$ meV, $M^{(1)}_\lambda = 50$ meV, $M^{(2)}_\lambda = -2$ meV, $\gamma_{\rm ph} = 1$ meV). The inset in (b) depicts the eh-pair processes dominating the damping rate. (c) Nonequilibrium excitation $\tilde{n}_\lambda$ of the renormalized vibration calculated using Eq. (4) (solid lines) and the rate-equation result in Eq. (6) (black dashed lines). (d) Electronic current through the junction.

underlines the importance of the $\gamma_{\rm ph}$ parameter for vibrational heating and instabilities[6,7,40] in nanoscale junctions.

OPV3 junction. In the remaining part of the Rapid Communication, we present first-principles based calculations of the carrier-induced frequency renormalization and vibrational heating in a junction based on the amine-terminated oligo(3)-phenylenevinylene (OPV3) molecule [see Fig. 1(a)], where frequency shifts of the order of $\sim$1 meV, spectral broadening, and significant heating have been observed experimentally with increasing bias voltage.[4] The frequency shifts were so far ascribed[4] to a vibrational Stark effect.[41] However, calculations of ours of the vibrational frequencies in the presence of an electric field do not support this interpretation.[34]

In our model of the OPV3 junction, transport through the LUMO of the OPV3 molecule positioned off resonant ($\varepsilon_0 = 0.5$ eV) with respect to the equilibrium chemical potentials of the leads ($\mu_{L/R} = \pm V/2$) and coupled symmetrically to the contacts ($\Gamma_{L/R} = 0.2$ eV) is assumed.[42] The next molecular level lies $\sim$1 eV above the LUMO and can hence be neglected. The vibrations and el-vib interactions have been obtained from first principles for the isolated OPV3 molecule,[34] thus neglecting direct effects from the leads. With few exceptions, the quadratic couplings, which are of the order of $|M^{(2)}_{\lambda\lambda'}| \sim$ 0–10 meV, are found to be negative, corresponding to frequency softening upon charging of the LUMO. This is in good agreement with a recent study of charging-induced frequency shifts in molecular junctions.[43]

Figure 3 shows the bias dependence of the vibrational spectral function $A(\omega)$ for the OPV3 junction. We focus here

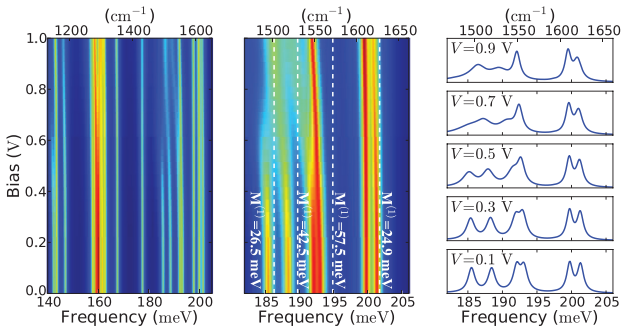

FIG. 3. (Color online) Vibrational spectral function $A(\omega)$ for the amine-terminated OPV3 molecule as a function of bias voltage. In the magnified center plot, the unperturbed frequencies ω_λ of the isolated molecule (vertical dashed lines) and the linear el-vib couplings $M_\lambda^{(1)}$ are indicated for the modes with the strongest el-vib interaction. Only the projection of the spectral function onto vibrations with significant el-vib coupling ($|M_\lambda^{(1)}| > 5$ meV) is shown.

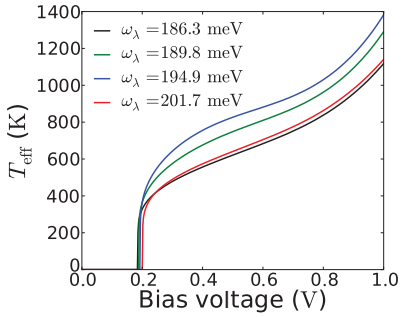

FIG. 4. (Color online) Effective nonequilibrium temperature $T_{\rm eff}$ from Eq. (6) ($\gamma_{\rm ph} = 1$ meV) for the OPV3 modes marked with dashed lines in the center panel of Fig. 3.

on the high-energy vibrations ($\omega_\lambda > 140$ meV), but note that the low-energy part of the spectral function shows a similar bias dependence.[34] Overall, the calculated spectral function reproduces[44] the features in the Raman spectra of Fig. 3(b) of Ref. 4. The spectral lines show clear mode *softening* of up to ∼2 meV with increasing bias voltage (for HOMO dominated transport, however, many of the spectral lines show mode *hardening*[34]). This is a result of partial charging and screening that follows as the chemical potential of the left lead moves into the broadened LUMO resonance. The relative magnitude of the two effects is sensitive to the level alignment and lead broadening in the junction. Here, they contribute comparably to the frequency renormalization. The eh-pair damping that accompanies screening gives rise to pronounced broadening of some of the spectral lines. This effect correlates with the strength of the linear el-vib interaction $M_\lambda^{(1)}$, which is indicated in the center panel of Fig. 3 for the modes with the strongest interaction. At zero bias, the spectral peaks for these modes are shifted from the frequencies of the isolated molecule (vertical dashed lines) due to (equilibrium) charging and screening. At large bias voltages, el-vib mediated mode-mode couplings result in a nontrivial bias dependence of some of the closely lying spectral lines.

In Fig. 4 we show the *effective* nonequilibrium temperature $T_{\rm eff}$ from Eq. (6) for the OPV3 modes marked with dashed lines in the center panel of Fig. 3. Above the emission threshold at $eV = \hbar\tilde{\omega}_\lambda$, the temperature of the vibrations jumps to several hundred Kelvin. For the $\omega_\lambda = 201.7$ meV mode, the temperature is in good agreement with the one for the mode with similar energy reported in Fig. 3(a) of Ref. 4. Comparing to Fig. 2(c), the approximate linear increase in the effective temperatures above the emission threshold is seen to correspond to the initial nonlinear increase in the occupation.

Conclusions. In summary, we have studied carrier-induced vibrational frequency renormalization, damping, and heating originating from the microscopic eh-pair excitation processes governing these observables. In junctions characterized by $\Gamma \lesssim \varepsilon_0, V$ where the effects are most pronounced, a strong correlation with nonlinear vibrational heating and the onset of current results (see Fig. 2). Such heating is inherent to junctions where the current is carried by a full electronic resonance and underlines the importance of eh-pair processes for the damping of vibrational heating. We have further shown that the voltage dependence of the Raman shifts and linewidths observed for an OPV3 molecular junction in Ref. 4 is not consistent with the originally proposed static Stark shift but can be explained by carrier-induced charging and screening effects.

Acknowledgments. We thank M. Galperin for fruitful discussions. The research of A.N. is supported by the Israel Science Foundation, the Israel-US Binational Science Foundation, and the European Research Council under the European Union's Seventh Framework Program (FP7/2007-2013; ERC Grant Agreement No. 226628). T.N. acknowledges financial support from the Czech Science Foundation via Grant No. 204/12/0897 and K.K. support from the Villum Kann Rasmussen Foundation.

*cosby@fys.ku.dk

[1] Z. Huang, F. Chen, R. D'agosta, P. A. Bennett, M. Di Ventra, and N. Tao, Nat. Nanotechnol. **2**, 698 (2007).

[2] G. Schulze, K. J. Franke, A. Gagliardi, G. Romano, C. S. Lin, A. L. Rosa, T. A. Niehaus, T. Frauenheim, A. Di Carlo, A. Pecchia, and J. I. Pascual, Phys. Rev. Lett. **100**, 136801 (2008).

[3] Z. Ioffe, T. Shamai, A. Ophir, G. Noy, I. Yutsis, K. Kfir, O. Cheshnovsky, and Y. Selzer, Nat. Nanotechnol. **3**, 727 (2008).

[4] D. R. Ward, D. A. Corley, J. M. Tour, and D. Natelson, Nat. Nanotechnol. **6**, 33 (2011).

[5] M. Galperin, M. A. Ratner, and A. Nitzan, J. Phys.: Condens. Matter **19**, 103201 (2007).

[6] R. Härtle and M. Thoss, Phys. Rev. B **83**, 125419 (2011).

[7] J.-T. Lü, P. Hedegård, and M. Brandbyge, Phys. Rev. Lett. **107**, 046801 (2011).

[8] M. Galperin, K. Saito, A. V. Balatsky, and A. Nitzan, Phys. Rev. B **80**, 115427 (2009).

[9] G. Romano, A. Gagliardi, A. Pecchia, and A. Di Carlo, Phys. Rev. B **81**, 115438 (2010).

[10] R. Härtle and M. Thoss, Phys. Rev. B **83**, 115414 (2011).

[11]D. Dundas, E. J. McEniry, and T. N. Todorov, Nat. Nanotechnol. **4**, 99 (2009).
[12]J.-T. Lü, M. Brandbyge, and P. Hedegård, Nano Lett. **10**, 1657 (2010).
[13]N. Bode, S. V. Kusminskiy, R. Egger, and F. von Oppen, Phys. Rev. Lett. **107**, 036804 (2011).
[14]J.-T. Lü, M. Brandbyge, P. Hedegård, T. N. Todorov, and D. Dundas, Phys. Rev. B **85**, 245444 (2012).
[15]M. Paulsson, T. Frederiksen, and M. Brandbyge, Phys. Rev. B **72**, 201101 (2005); T. Frederiksen, M. Paulsson, M. Brandbyge, and A.-P. Jauho, *ibid*. **75**, 205413 (2007).
[16]T. Novotný, F. Haupt, and W. Belzig, Phys. Rev. B **84**, 113107 (2011).
[17]Y. Utsumi, O. Entin-Wohlman, A. Ueda, and A. Aharony, Phys. Rev. B **87**, 115407 (2013).
[18]M. Galperin, M. A. Ratner, and A. Nitzan, Nano Lett. **9**, 758 (2009).
[19]M. Galperin, M. A. Ratner, and A. Nitzan, J. Chem. Phys. **130**, 144109 (2009).
[20]S. Pisana, M. Lazzeri, C. Casiraghi, K. S. Novoselov, A. K. Geim, A. C. Ferrari, and F. Mauri, Nat. Mater. **6**, 198 (2007).
[21]J. Yan, Y. Zhang, P. Kim, and A. Pinczuk, Phys. Rev. Lett. **98**, 166802 (2007).
[22]G. A. Steele, A. K. Hüttel, B. Witkamp, M. Poot, H. B. Meerwaldt, L. P. Kouwenhoven, and H. S. J. van der Zant, Science **325**, 1103 (2009).
[23]B. Lassagne, Y. Tarakanov, J. Kinaret, D. Garcia-Sanchez, and A. Bachtold, Science **325**, 1107 (2009).
[24]H. B. Meerwaldt, G. Labadze, B. H. Schneider, A. Taspinar, Y. M. Blanter, H. S. J. van der Zant, and G. A. Steele, Phys. Rev. B **86**, 115454 (2012).
[25]M. Ganzhorn and W. Wernsdorfer, Phys. Rev. Lett. **108**, 175502 (2012).
[26]H. Haug and A.-P. Jauho, *Quantum Kinetics in Transport and Optics of Semiconductors* (Springer, Berlin, 1998).
[27]J. K. Viljas, J. C. Cuevas, F. Pauly, and M. Häfner, Phys. Rev. B **72**, 245415 (2005).
[28]M. Galperin, M. A. Ratner, and A. Nitzan, J. Chem. Phys. **121**, 11965 (2004).
[29]In practical calculations, the self-energy in Eq. (1) should not include effects already accounted for in the *bare* frequencies ω_λ. For example, in first-principles calculations of vibrational frequencies in nanoscale junctions within the Born-Oppenheimer approximation (Ref. 15), the frequencies ω_λ calculated at zero bias include the static screening and charging of the equilibrium configuration. The electronic self-energy $\Pi^{\rm el} = \Pi^{(1)} + \Pi^{(2)}$ [Eqs. (2) and (3)] must therefore be corrected according to $\Pi^{\rm el}(\omega, V) \to \Pi^{\rm el}(\omega, V) - \Pi^{\rm el}(\omega = 0, V = 0)$, where $\Pi^{\rm el}(\omega = 0, V = 0)$ is the static zero-bias self-energy, in order not to double count these contributions.
[30]N. Mingo, Phys. Rev. B **74**, 125402 (2006).
[31]A. Pecchia, G. Romano, and A. Di Carlo, Phys. Rev. B **75**, 035401 (2007).
[32]M. Engelund, M. Brandbyge, and A.-P. Jauho, Phys. Rev. B **80**, 045427 (2009).
[33]S. Kim and N. Marzari, Phys. Rev. B **87**, 245407 (2013).
[34]See Supplemental Material at http://link.aps.org/supplemental/10.1103/PhysRevB.88.201405 for the details of the theory and the first-principles calculations.
[35]T. Frederiksen, M. Brandbyge, N. Lorente, and A.-P. Jauho, Phys. Rev. Lett. **93**, 256601 (2004).
[36]D. F. Urban, R. Avriller, and A. Levy Yeyati, Phys. Rev. B **82**, 121414(R) (2010).
[37]D. Djukic, K. S. Thygesen, C. Untiedt, R. H. M. Smit, K. W. Jacobsen, and J. M. van Ruitenbeek, Phys. Rev. B **71**, 161402 (2005).
[38]In spite of the nonconservative nature of the first Born approximation applied here, it is expected to give a quantitative description of vibrational heating in the regime of weak el-vib interaction (Ref. 39).
[39]J.-T. Lü and J.-S. Wang, Phys. Rev. B **76**, 165418 (2007).
[40]T. Gunst, J.-T. Lü, P. Hedegård, and M. Brandbyge, Phys. Rev. B **88**, 161401 (2013).
[41]D. K. Lambert, Solid State Commun. **51**, 297 (1984).
[42]Our choice of parameters for the OPV3 junction corresponds to a zero-bias conductance of $G \sim 0.1 G_0$ ($G_0 = 2e^2/h$), which is slightly larger than the conductance values reported in Ref. 4.
[43]F. Mirjani, J. M. Thijssen, and M. A. Ratner, J. Phys. Chem. C **116**, 23120 (2012).
[44]Note that the cross section for Raman scattering is mode dependent, implying that not all spectral lines show up in Raman spectroscopy.